

# Tevatron luminosity with beam-beam interactions and self-consistent optics

T. Sen

Fermilab, P.O. Box 500, Batavia, IL, 60510

B. Anhalt

University of Kansas, Lawrence, KA

## Abstract

Beam-beam effects change the closed orbits and other optics functions of both protons and anti-protons. We calculate the self-consistent optics of both beams at full intensity and their impact on luminosity in the Tevatron.

## 1 Introduction

Optics changes at the collision point impact the luminosity. Long-range beam-beam interactions change the closed orbit of both protons and anti-protons in the Tevatron. Consequently they also change the transverse offsets and the crossing angles at the experimental collision points at B0 and D0 and reduce the luminosity. Both head-on collisions and long-range interactions induce a beta-beating which can change the rms beam sizes at B0 and D0. This so called 'dynamic beta effect' can either increase or decrease the luminosity depending on the sign of the change in  $\beta^*$ . We report on the impact of these geometrical effects on the luminosity with a self-consistent calculation of the optics changes in both beams induced by the beam-beam interactions. Intensities are taken to be at their maximum design values. Earlier theoretical studies, see e.g [1], have mostly focused on beam-beam effects on the anti-protons.

Aside from these geometric effects, dynamical effects due to the beam-beam interactions also influence the luminosity. These effects will be more severe when both beams are at their maximum intensity. In this "strong-strong" regime the dynamical effects may range from emittance growth to particle loss due to coherent instabilities. Insight into the coherent modes can be gained by a perturbative analysis of the Vlasov equation but typically detailed numerical simulations are required to observe the full range of phenomena. We will not discuss such effects here.

## 2 Self-consistent calculation of orbits and Twiss functions

The optics with beam-beam effects is calculated iteratively using the program MAD. The lattice description includes the known machine nonlinearities and the beam-beam elements for each bunch.

	Protons	Anti-protons
Bunch intensity [ $\times 10^{11}$ ]	2.7	1.27
Transverse emittance [mm-mrad]	20	15
Momentum spread [ $\times 10^{-4}$ ]	1.3	1.3

Table 1: Design values of selected beam parameters at 980 GeV

In the absence of the beam-beam effects, all bunches in a beam (proton or anti-proton) follow the same closed orbit. The beam-beam effects introduce changes in orbits, beta functions, dispersion functions, tunes etc. which are different for each bunch.

At collision each bunch experiences 72 beam-beam interactions including two head-on collisions at B0 and D0. Around the ring there are 138 different locations for the interactions and each bunch sees a different sequence of 72 interactions amongst these 138 interactions. Consequently beam-beam effects vary from bunch to bunch. If all bunch parameters in a beam (e.g. intensities and emittances) are the same, we can assume three-fold symmetry in a beam so that bunch to bunch changes within a train are the same in all 3 trains. We will assume three-fold symmetry in this report.

The collision sequence is such that anti-proton bunch A1 collides with proton bunch P13 at B0, and with proton bunch P25 at D0. Similarly P1 collides with bunch A25 at B0 and bunch A13 at D0. Appendix A shows the collision configuration in more detail. With three-fold symmetry, bunch numberings can be limited to the range 1-12. It is straightforward to relax this assumption of 3-fold symmetry if necessary.

The self-consistent algorithm starts with the calculation of the anti-proton optics using the unperturbed optics on the proton helix. The optics calculation for a single anti-proton bunch requires the closed orbits, intensities and rms sizes of the 12 proton bunches at the 72 specific locations where this anti-proton bunch meets the opposing proton bunches. This is repeated for all 12 anti-proton bunches. The revised optics for each anti-proton bunch is used to update the anti-proton closed orbit and transverse rms size at each interaction location. At the next step of the iterative process, the closed orbits, beta functions, dispersions etc. of the proton bunches are calculated using the updated anti-proton parameters. At the end of this step, proton bunch parameters at all interaction locations are updated. The procedure is repeated until the calculations converge to a specified precision. We find that typically 3 iterations for each beam suffice for convergence.

### 3 Optics and Luminosities with uniform beam parameters

First we calculate the optics changes with the design values of the beam parameters. Table 1 shows the values of some key parameters at 980 GeV. In this section we assume that all bunches in a beam have the same values of the parameters. In the next section we consider a case with varying bunch parameters typical of a store.

As an example the changes in closed orbits at the beam-beam interaction locations for anti-proton bunch 6 and proton bunch 6 are shown in Figure 1. The rms change in anti-proton orbits is roughly  $0.2\sigma$  in both planes and is nearly the same for all anti-proton bunches. The rms change in

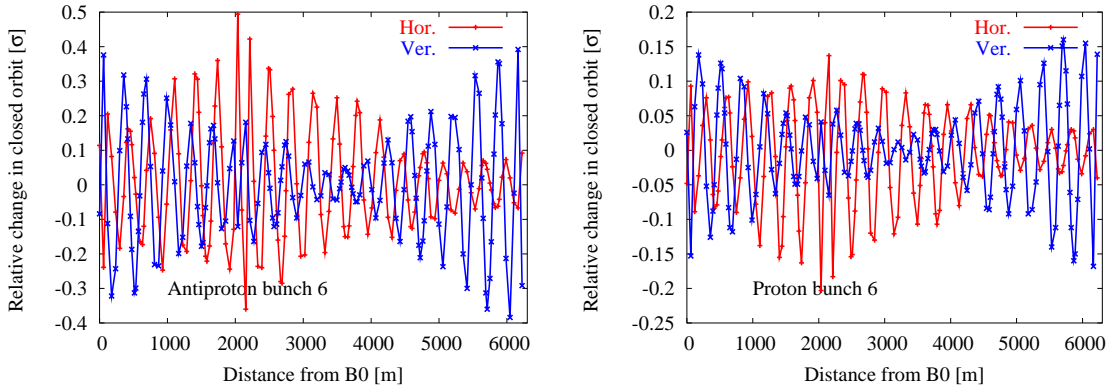


Figure 1: Change in the closed orbits (in units of rms beam size) at all interaction points due to the beam-beam interactions. B0 is at 0 m while D0 is at 2094 m. Left: Anti-proton bunch 6, Right: Proton bunch 6

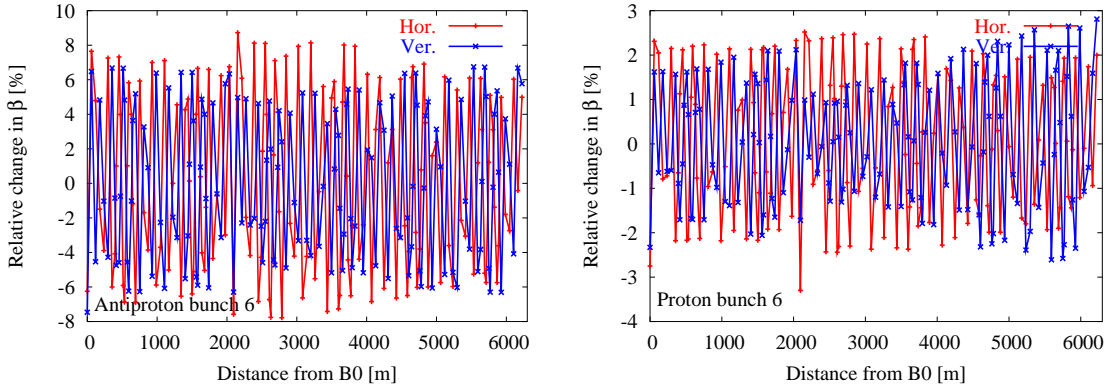


Figure 2: Relative change in the beta functions (in %) at all interaction points due to the beam-beam interactions. Left: Anti-proton bunch 6, Right: Proton bunch 6

proton orbits is roughly  $0.07\sigma$  in both planes and is also nearly uniform over all the proton bunches. Figure 2 shows the beta beating for the same two bunches also at the beam-beam interactions. The beta-beat oscillates at twice the betatron frequency, thus 41 periods are visible in these plots. The beta-beating is significant for anti-protons, with a maximum around 8% for bunches 2 to 11 but higher for bunches 1 and 12. The maximum beta-beating is around 3% for proton bunches 2-11 but higher for bunches 1 and 12. It turns out that the maximum beta beating for both beams occur either at B0 or D0 or at one of the neighbouring parasitic locations. This beta-beating therefore strongly influences the luminosity. It also affects the calibration of instruments such as flying wires that rely on lattice function measurements.

Figure 3 shows the maximum of the orbit changes over all the anti-proton and proton bunches. The maximum for the anti-protons ranges from  $0.3$ - $0.6\sigma$  which at 980 GeV is not large in absolute size at most locations. Maximum changes for proton bunches are a factor of 2-3 smaller.

The maximum changes in beta functions are shown in Figure 4. The beta beating is very large

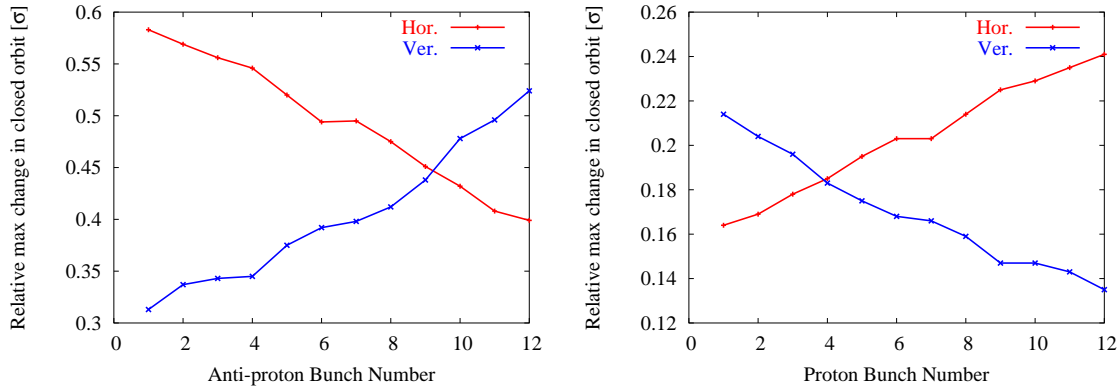


Figure 3: Maximum absolute change in the closed orbits (in units of rms beam size) at all interaction points due to the beam-beam interactions for 12 bunches. Left: Anti-proton bunches, Right: Proton bunches

for outlier bunches 1 and 12 in both beams. The maximum changes in the dispersion functions, seen in Figure 5, are of the order of a few cm for both beams and do not influence the beam sizes much. The changes in the dispersion functions could also influence the synchro-betatron effects from the beam-beam interactions but again not significantly since the changes are small.

The most important changes in the beta functions are those which occur at B0 and D0. Figures 6 and 7 show the relative changes at B0 and D0 for both beams. We observe that the dynamic beta-beating has a positive impact on the luminosity since it reduces the beta functions at both collision points for both beams. Recent estimates of  $\beta^*$  from the luminous region have yielded values smaller than the 35 cm value expected from linear optics. The largest reductions occur for the outlier bunches 1 and 12 in both beams - the luminosity of these bunches should therefore benefit the most.

Figures 8 and 9 show the offsets and crossing angles respectively. At B0 the horizontal offsets are somewhat larger than the vertical offsets while at D0, the reverse is true on average. The vertical crossing angles are larger than the horizontal crossing angles at B0 while again the reverse is true at D0. The small spread in offsets and crossing angles over the bunches implies that the luminosity reduction will be small if the average offsets and crossing angles are corrected.

The zero amplitude tune shifts and chromaticities for individual anti-proton and proton bunches due to the beam-beam interactions are shown in Figures 10 and 11 respectively. We observe the characteristic pattern of tune variation in anti-proton bunches expected from earlier studies and recent measurements. The proton tune shifts are slightly less than a factor of two smaller, as expected from the ratio of intensities to emittances. It is interesting that the change in the horizontal chromaticities of protons due to the beam-beam interactions are of nearly the same magnitude as the change in chromaticities of anti-protons. These values also suggest that during collision, the horizontal chromaticity on the anti-proton helix has to be greater than 7 units and greater than 5 units on the proton helix in order to avoid the head-tail instability.

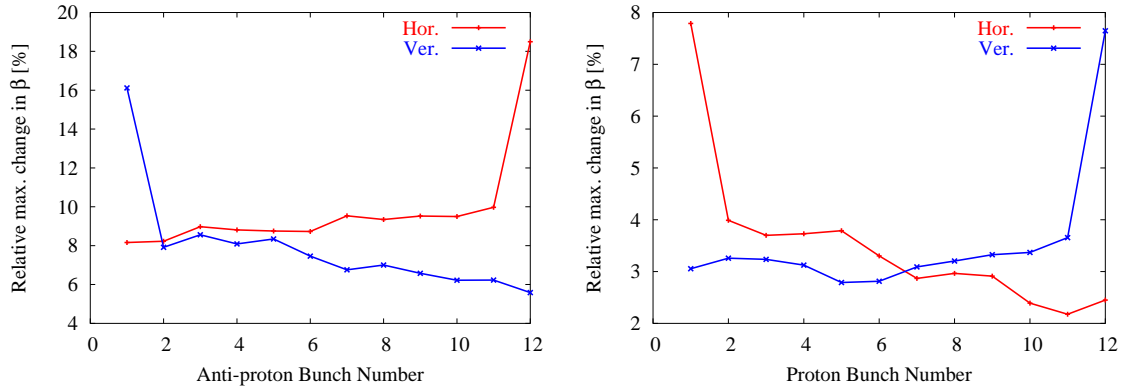


Figure 4: Maximum of the absolute relative change in the beta functions (in %) at all interaction points due to the beam-beam interactions for 12 bunches. Left: Anti-proton bunches, Right: Proton bunches

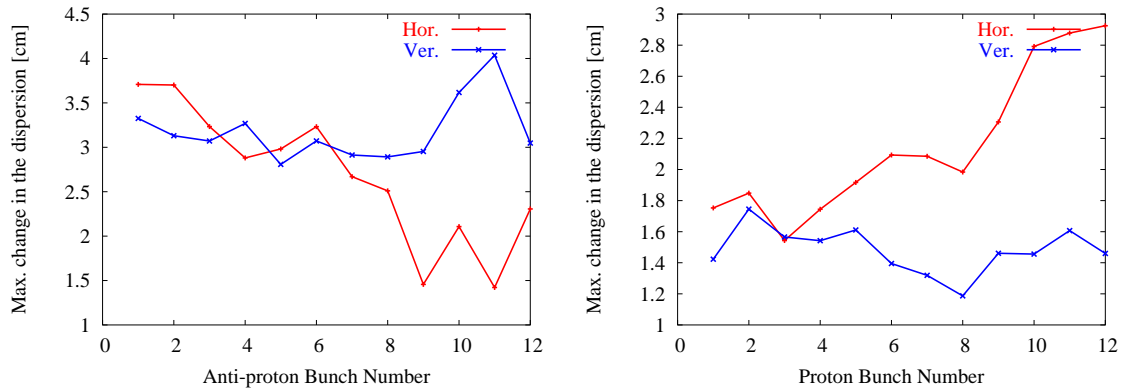


Figure 5: Maximum change in the dispersion functions (in cm) at all interaction points due to the beam-beam interactions for 12 bunches. Left: Anti-proton bunches, Right: Proton bunches

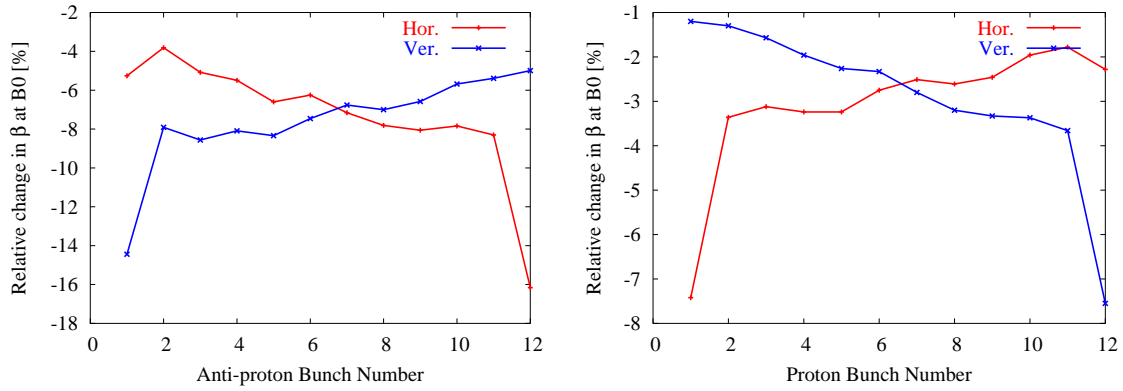


Figure 6: Relative change in the beta functions (in %) at B0 due to the beam-beam interactions for all the 12 bunches. Left: Anti-proton bunches, Right: Proton bunches. The beta functions are smaller at B0 because of the beam-beam interactions.

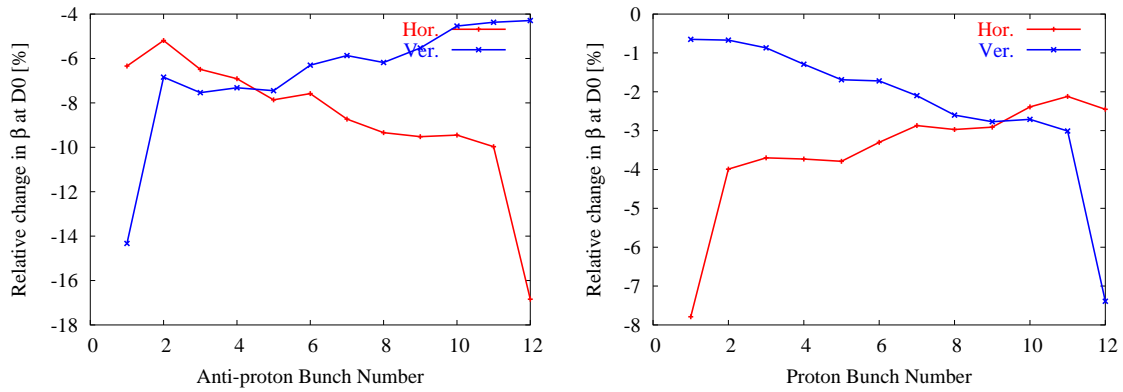


Figure 7: Relative change in the beta functions (in %) at D0 due to the beam-beam interactions for all the 12 bunches. Left: Anti-proton bunches, Right: Proton bunches

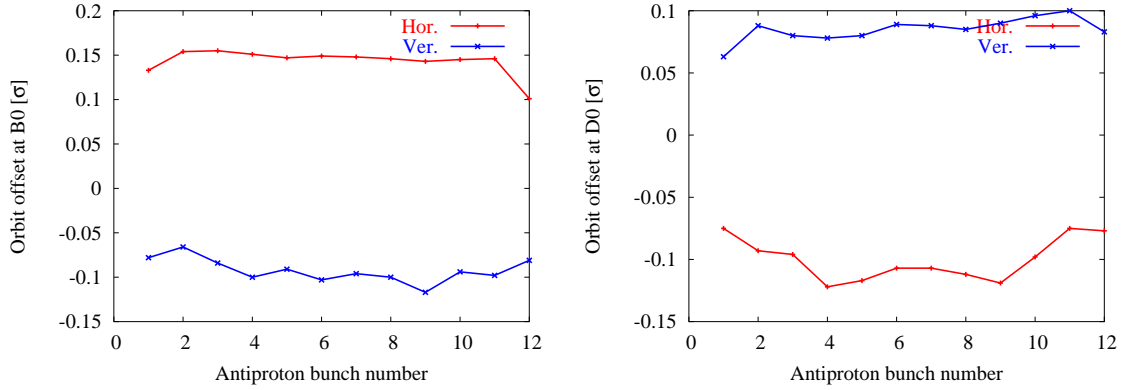


Figure 8: Offsets between the colliding bunches (in units of the rms size) at the collision points. Left: B0, Right: D0. The standard deviation of the offsets at B0 are  $0.014\sigma$  in both planes while at D0 the standard deviations are  $(0.017, 0.009)\sigma$ .

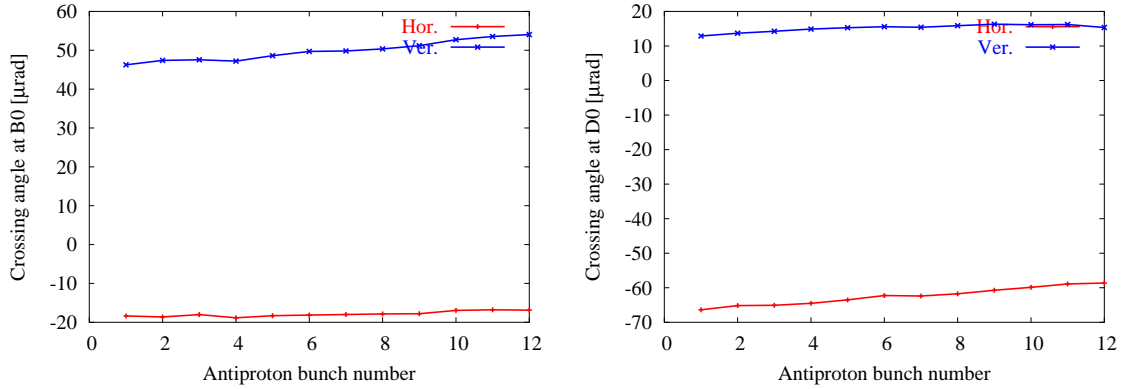


Figure 9: Crossing angles between the colliding bunches (in micro-radians) at the collision points. Left: B0, Right: D0. The standard deviation of the crossing angles at B0 are  $(0.7, 2.6)$  micro-rad while at D0 the standard deviations in crossing angles are  $(2.6, 1.1)$  micro-rad.

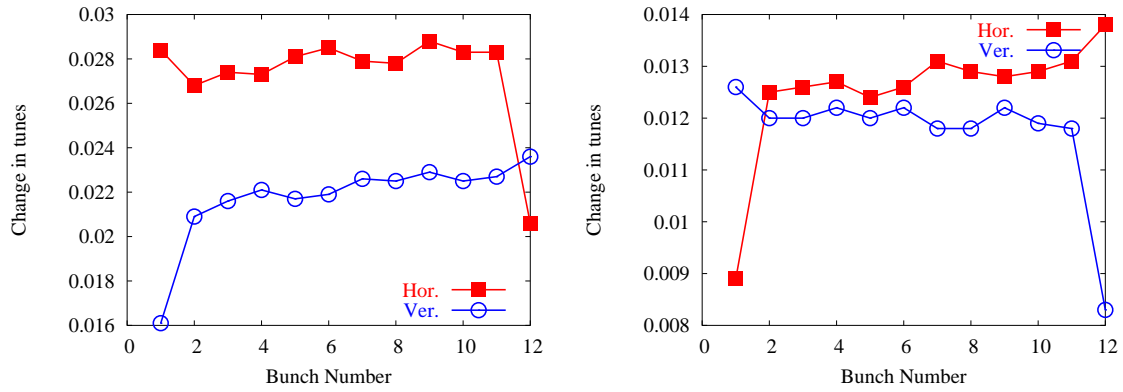


Figure 10: Zero amplitude tune shifts due to the beam-beam interactions. Left: anti-protons, Right: protons.

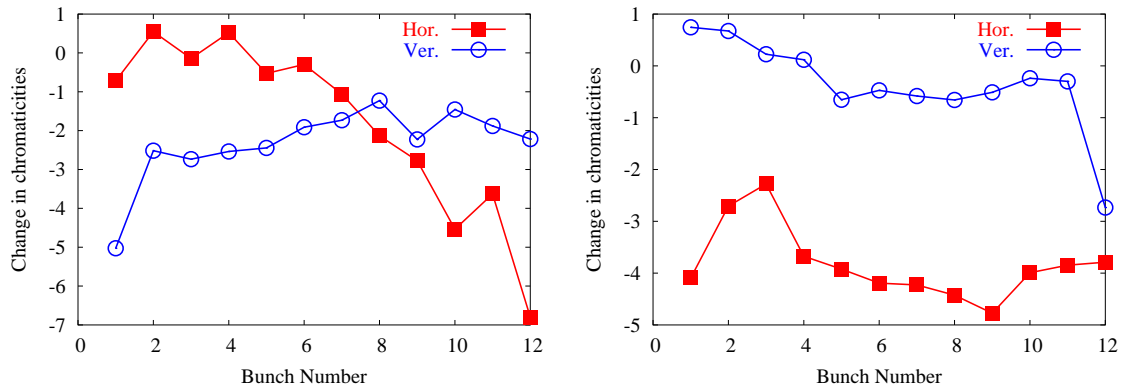


Figure 11: Zero amplitude chromaticity shifts due to the beam-beam interactions. Left: anti-protons, Right: protons.

The change in luminosity can be found once the beam sizes, offsets and crossing angles are known. The bunch luminosity is given by

$$\mathcal{L} = \frac{1}{4\pi} \frac{N_P N_A f_{rev}}{\sqrt{2\pi}} \int_{-\infty}^{\infty} \frac{dt}{\sigma_x \sigma_y} \exp\left[-\frac{t^2}{2} - \frac{\Delta x^2}{4\sigma_x^2} - \frac{\Delta y^2}{4\sigma_y^2}\right] \quad (1)$$

where

$$\begin{aligned} \sigma_x^2 &= \frac{1}{2} \left\{ \beta_{x,P}^* \epsilon_{x,P} [1 - 2 \frac{\alpha_{x,P}^*}{\beta_{x,P}^*} \sigma_z t + (1 + (\alpha_{x,P}^*)^2) (\frac{\sigma_z t}{\beta_{x,P}^*})^2] + [D_{x,P}^* (1 + \frac{D'_{x,P}}{D_{x,P}^*} \sigma_z t) \delta_{p,P}]^2 \right. \\ &\quad \left. + \beta_{x,A}^* \epsilon_{x,A} [1 - 2 \frac{\alpha_{x,A}^*}{\beta_{x,A}^*} \sigma_z t + (1 + (\alpha_{x,A}^*)^2) (\frac{\sigma_z t}{\beta_{x,A}^*})^2] + [D_{x,A}^* (1 + \frac{D'_{x,A}}{D_{x,A}^*} \sigma_z t) \delta_{p,A}]^2 \right\} \\ \sigma_y^2 &= \frac{1}{2} \left\{ \beta_{y,P}^* \epsilon_{y,P} [1 - 2 \frac{\alpha_{y,P}^*}{\beta_{y,P}^*} \sigma_z t + (1 + (\alpha_{y,P}^*)^2) (\frac{\sigma_z t}{\beta_{y,P}^*})^2] + [D_{y,P}^* (1 + \frac{D'_{y,P}}{D_{y,P}^*} \sigma_z t) \delta_{p,P}]^2 \right. \\ &\quad \left. + \beta_{y,A}^* \epsilon_{y,A} [1 - 2 \frac{\alpha_{y,A}^*}{\beta_{y,A}^*} \sigma_z t + (1 + (\alpha_{y,A}^*)^2) (\frac{\sigma_z t}{\beta_{y,A}^*})^2] + [D_{y,A}^* (1 + \frac{D'_{y,A}}{D_{y,A}^*} \sigma_z t) \delta_{p,A}]^2 \right\} \\ \sigma_z^2 &= \frac{1}{2} (\sigma_{z,P}^2 + \sigma_{z,A}^2) \\ \Delta x &= \Delta x_0 + \Delta x'_0 \sigma_z t \\ \Delta y &= \Delta y_0 + \Delta y'_0 \sigma_z t \end{aligned} \quad (2)$$

$\Delta x_0, \Delta y_0$  and  $\Delta x'_0, \Delta y'_0$  are the beam offsets and crossing angles respectively. Other symbols have their usual meaning.

The luminosity is inversely proportional to the product of the rms sizes at the IP. It is instructive to calculate the change in  $1/[\sigma_x \sigma_y]$  at B0 and D0 due to the beta-beating. Figure 12 shows the relative change for the 12 bunches. This factor increases by about 4-5 % for bunches 2-11 while the increase for the outlier bunches is 7.5-8%.

We use Equation (1) to calculate the change in the specific luminosity, the luminosity without the bunch intensities. We assume that the average offset and crossing angles over all bunches are removed by properly adjusting the separator voltages. Thus the remaining bunch offsets and crossing angles are calculated as

$$\begin{aligned} \Delta x_0^{eff} &= \Delta x_0 - \langle \Delta x_0 \rangle, & \Delta x'_0{}^{eff} &= \Delta x'_0 - \langle \Delta x'_0 \rangle \\ \Delta y_0^{eff} &= \Delta y_0 - \langle \Delta y_0 \rangle, & \Delta y'_0{}^{eff} &= \Delta y'_0 - \langle \Delta y'_0 \rangle \end{aligned} \quad (3)$$

The averages  $\langle \rangle$  are taken over all bunches. We use the effective offsets ( $\Delta x_0^{eff}, \Delta y_0^{eff}$ ) and crossing angles ( $\Delta x'_0{}^{eff}, \Delta y'_0{}^{eff}$ ) in the calculation of the specific luminosity. Figure 13 shows the relative change in the specific luminosities when the dynamic beta-beating and effective offsets and crossing angles at the IPs are included. We observe that the pattern of the change in the specific luminosity over the different bunches follows the pattern of the increase in  $1/[\sigma_x \sigma_y]$  seen in Figure 12. Despite the offsets and crossing angles, there is a net increase of 2-3% in specific luminosity due to the beta-beating.

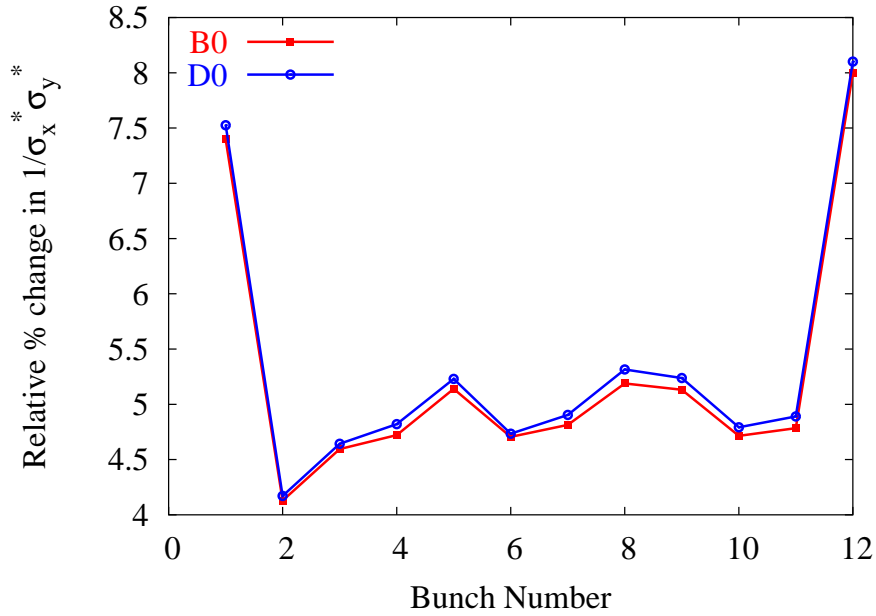


Figure 12: Relative % change in the inverse of the product of the rms spot sizes at the two collision points. The smaller beta functions at the IPs increase this factor by almost 5% for most bunches.

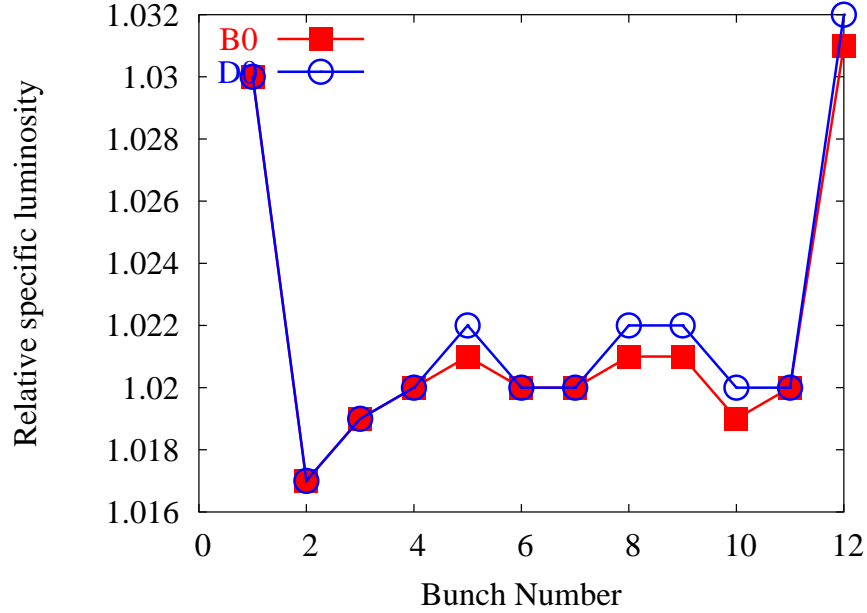


Figure 13: Relative specific luminosity at the two collision points. The smaller rms sizes at the IPs increase the luminosity while the offsets and crossing angles reduce the luminosity. Overall there is a small (2 - 3%) increase in luminosity due to the optics changes induced by the beam-beam interactions.

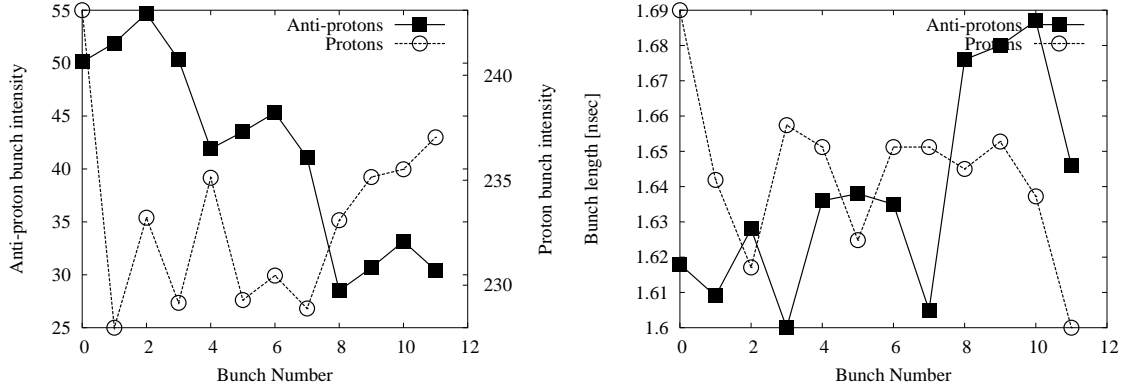


Figure 14: Intensities and bunch lengths averaged over the 3 trains at the start of Store 3925 (January 17, 2005).

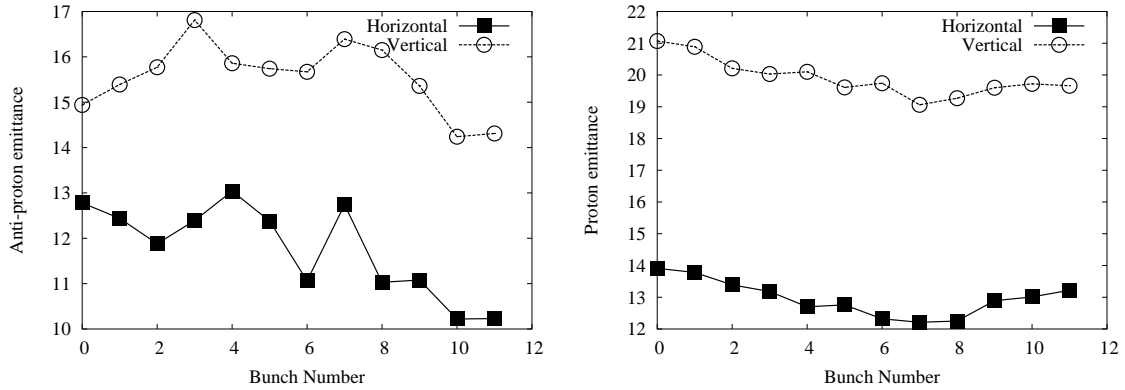


Figure 15: Anti-proton emittances (left) and proton emittances (right) averaged over the 3 trains at the start of Store 3925 (January 17, 2005).

## 4 Optics and Luminosities with non-uniform beam parameters

In this section we will consider the optics changes when the beam parameters vary from bunch to bunch as they do in a typical store. We take as an example Store 3925 on January 17, 2005 when the average initial luminosity was  $1.05 \times 10^{32} \text{ cm}^{-2} \text{ sec}^{-1}$ .

The range of variation in proton intensities is about 10% but it is about 100% for the anti-proton intensities. Bunch length variations are within 10% for both beams. The variation in anti-proton emittances is also larger than in proton emittances. We expect that this greater variation in bunch parameters will lead to a greater spread of optics changes, especially for the proton bunches.

We use the bunch lengths and emittances as shown in Figure 14 and 15. We use the same intensity variation as seen in Figure 14 but scale it so that the maximum proton bunch intensity is  $2.7 \times 10^{11}$  and the maximum anti-proton bunch intensity is  $1.27 \times 10^{11}$  - the values used in the previous section.

Figures 16 and 17 show the maximum relative changes in orbits and beta functions for the two beams. Compared to Figures 3 and 4, the scale of variations is the same but the pattern for the proton

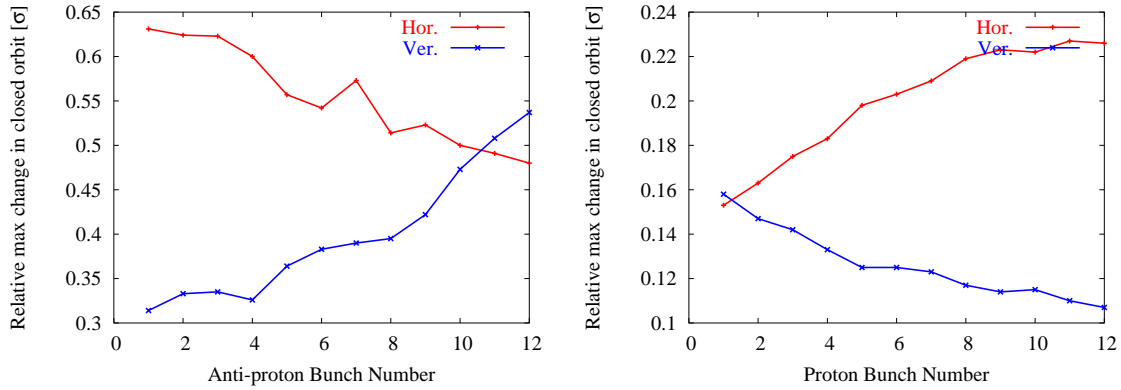


Figure 16: Maximum change in the closed orbits (in units of rms beam size) at all beam-beam interaction locations due to the beam-beam interactions for 12 bunches. Left: Anti-proton bunches, Right: Proton bunches

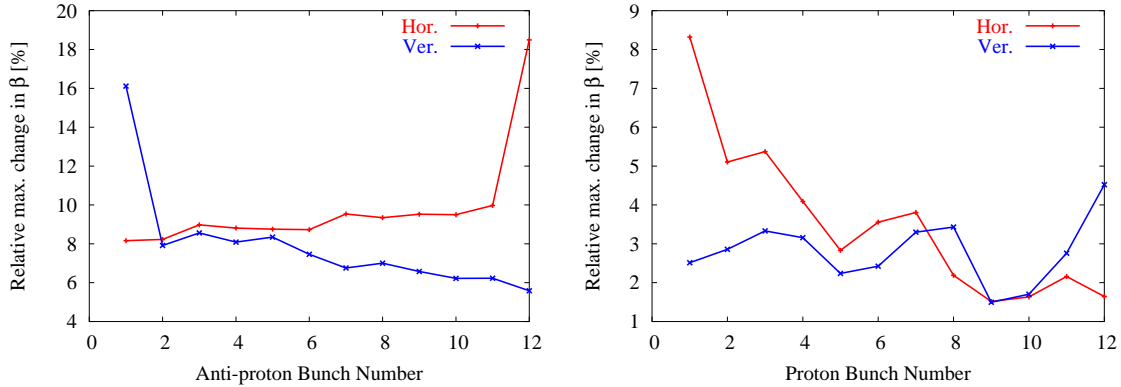


Figure 17: Maximum absolute relative change in the beta functions (in %) at all beam-beam interaction locations due to the beam-beam interactions for 12 bunches. Left: Anti-proton bunches, Right: Proton bunches

bunches follows the intensity pattern of the anti-proton bunches in Store 3925.

Figure 18 and 19 show the relative change in the beta functions at B0 and D0. Compared to Figures 6 and 7, the changes are of similar magnitude but again the pattern for proton bunches is influenced by the large variations in anti-proton intensities and emittances.

Figures 20 and 21 show the offsets and crossing angles at B0 and D0. These should be compared to Figures 8 and 9. The zero amplitude tune shifts and chromaticities are seen in Figures 22 and 23.

The relative change in  $1/[\sigma_x\sigma_y]$  at B0 and D0 is seen in Figure 24. Compared to Figure 12, the changes are similar except for bunch 12 which experiences a smaller reduction in the rms size. The relative specific luminosities calculated with the effective beam offsets and crossing angles is shown in Figure 25. We again observe a small net increase in luminosity due to the dynamic beta beating showing that this effect is robust against typical bunch to bunch variations in beam parameters.

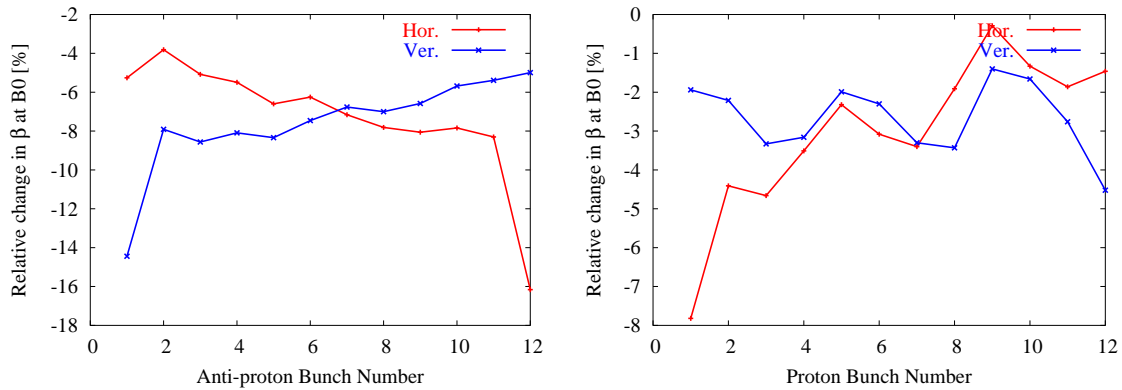


Figure 18: Relative change in the beta functions (in %) at B0 due to the beam-beam interactions for all the 12 bunches. Left: Anti-proton bunches, Right: Proton bunches

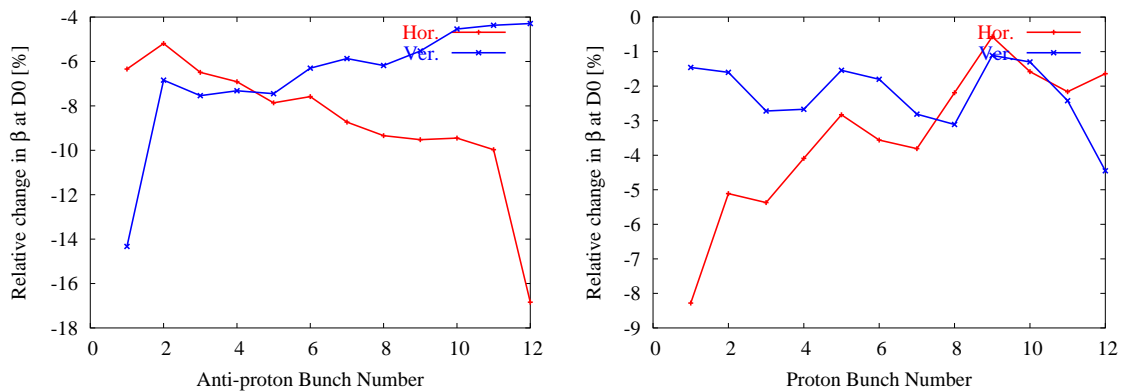


Figure 19: Relative change in the beta functions (in %) at D0 due to the beam-beam interactions for 12 bunches. Left: Anti-proton bunches, Right: Proton bunches

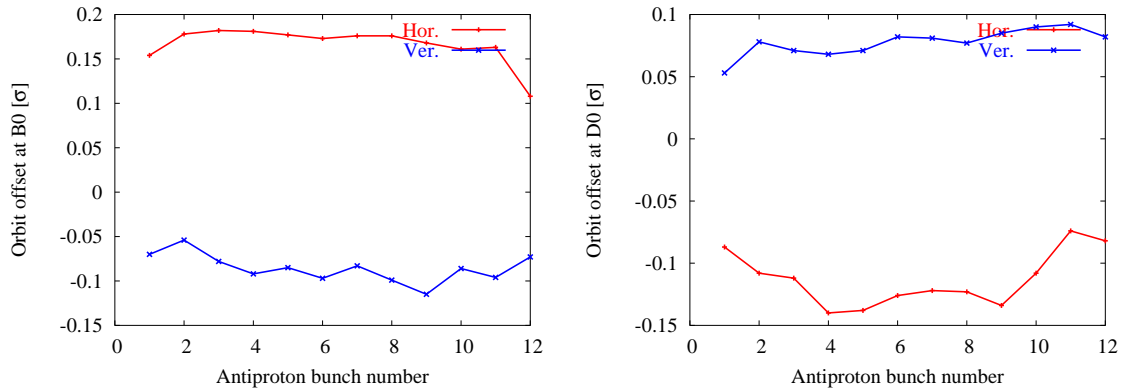


Figure 20: Offsets between the colliding bunches (in units of the rms size) at the collision points. Left: B0, Right: D0

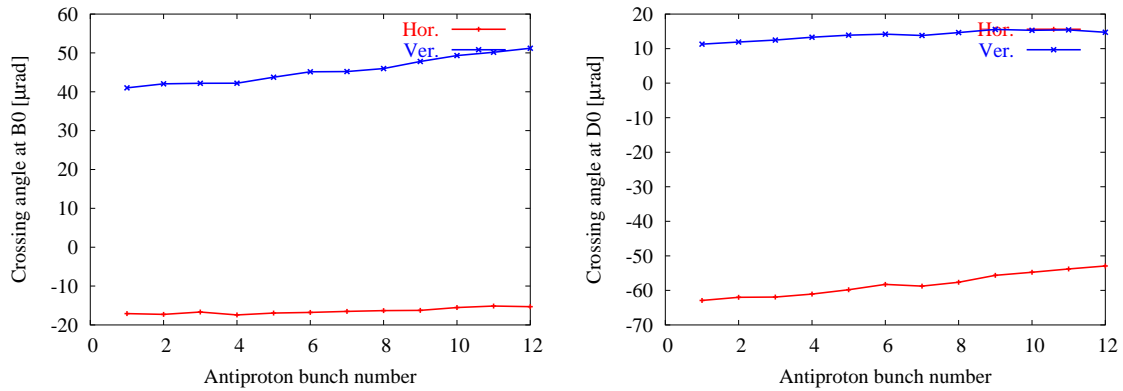


Figure 21: Crossing angles between the colliding bunches (in micro-radians) at the collision points. Left: B0, Right: D0

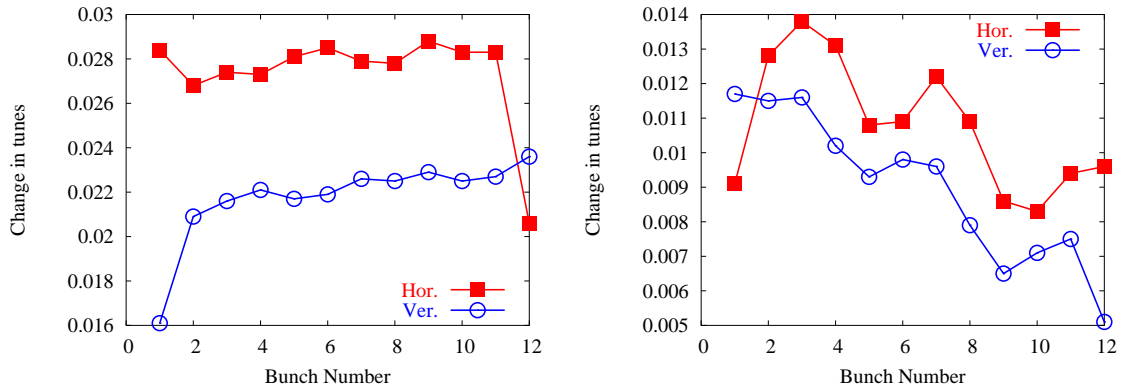


Figure 22: Zero amplitude tune shifts due to the beam-beam interactions. Left: anti-protons, Right: protons.

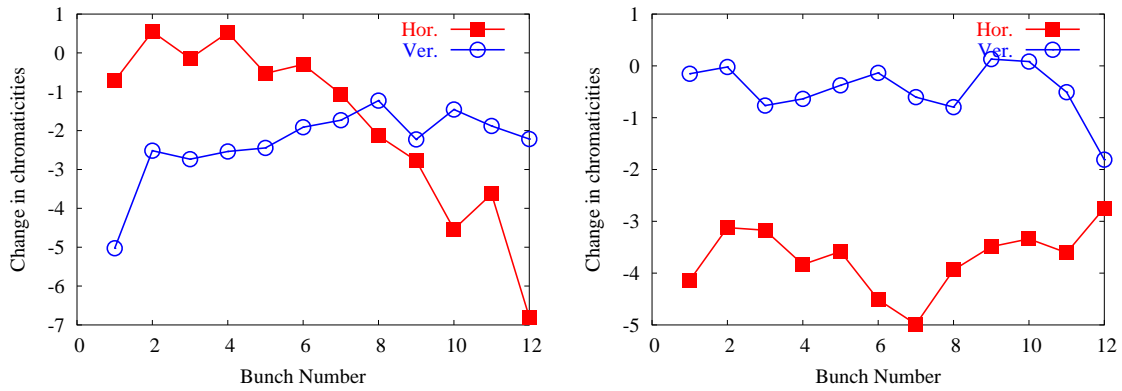


Figure 23: Zero amplitude chromaticity shifts due to the beam-beam interactions. Left: anti-protons, Right: protons.

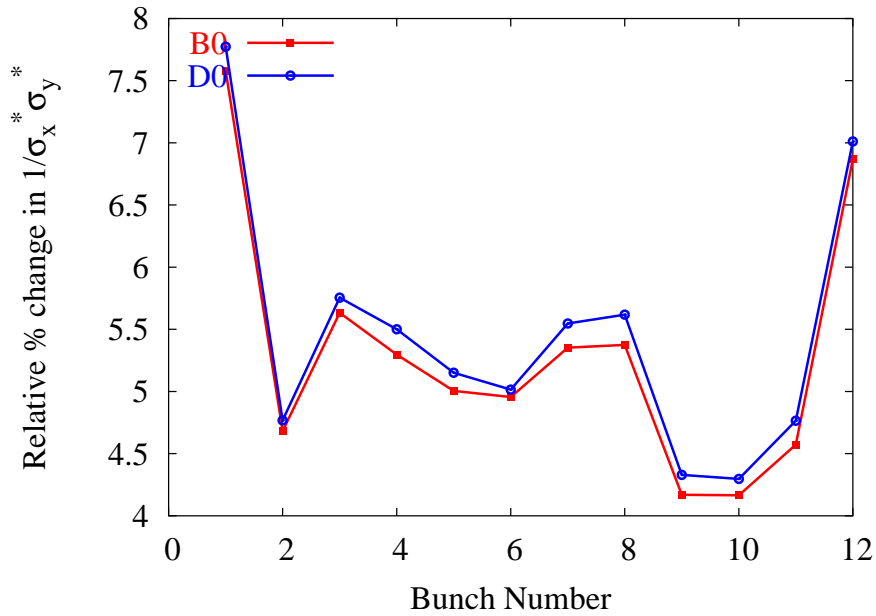


Figure 24: Relative % change in the inverse of the product of the rms spot sizes at the two collision points. The smaller beta functions at the IPs increase this factor by almost 5% for most bunches.

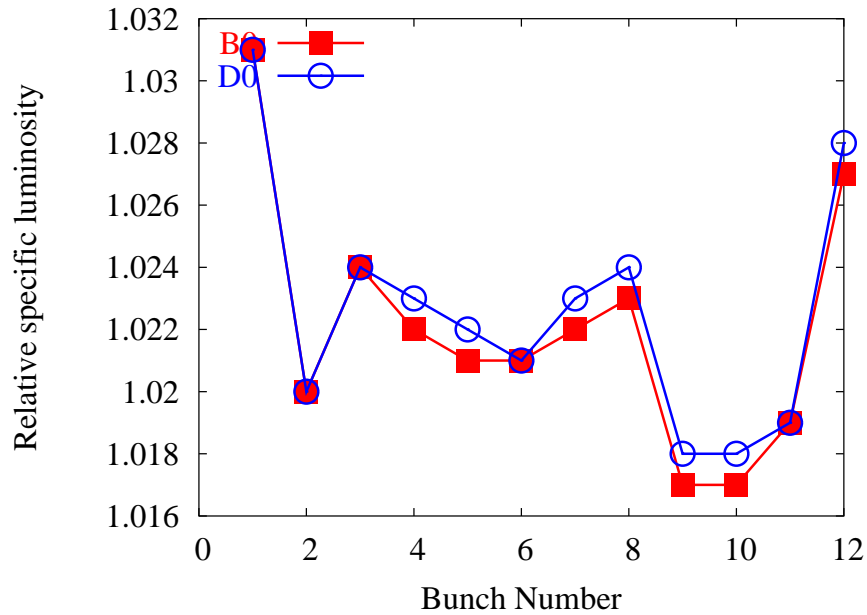


Figure 25: Relative specific luminosity at the two collision points. The smaller rms sizes at the IPs increase the luminosity while the offsets and crossing angles reduce the luminosity. Again there is a small increase in luminosity as also found with uniform beam parameters in the previous section.

## 5 Summary

- Beta-beating due to the beam-beam reduces the rms sizes at the collision points
- Offsets between beams at B0 and D0 are small, in the range of 0.05-0.15  $\sigma$ .
- Crossing angles between beams are about 20 micro-radians in one plane, 50 micro-radians in the other plane.
- Overall, because of the smaller spot sizes at B0 and D0, there is a slight increase ( $\sim$  1- 3%) in luminosity due to the beam-beam interactions. This net increase persists when typical bunch to bunch variations in beam parameters are included.

We also find that the specific luminosities of the outlier bunches 1 and 12 are slightly larger by 1% than that of the remaining bunches. This effect may be too small to be observable.

- Longer term dynamical effects - dynamic aperture, emittance growth, coherent instabilities etc. in this strong-strong regime have not been studied in this report.

## Acknowledgements

We thank Professor J. Shi for his support of Ben Anhalt.

## References

- [1] T. Sen, B. Erdelyi, M. Xiao, V. Boochoa, *Beam-beam effects at the Fermilab Tevatron: theory*, PRSTAB 7, 041001 (2004)

## Appendix A: Collision sequence

The bunches in the proton beam are numbered P1 to P36 while the anti-proton bunches are numbered A1 to A36. The bunches are numbered in the order of their injection. The injection process and this numbering sequence results in bunches P1 and A1 passing each other at F0.

The collision sequence at B0 and D0 for the three trains is

B0	D0
A1 - P13	A1 - P25
...	...
A12 - P24	A12 - P36
A13 - P25	A13 - P1
...	...
A24 - P36	A24 - P12
A25 - P1	A25 - P13
...	...
A36 - P12	A36 - P24

If we assume three-fold symmetry, then the bunch numbers can be restricted to modulo 12.